Chapter 20

Solar-Powered Micro-air Vehicles and Challenges in Downscaling

André Noth and Roland Siegwart

Abstract In many aerial vehicles applications, the flight duration is a key factor for the success of a mission. A solution to improve significantly this endurance is the use of solar energy. This chapter presents a conceptual design methodology for the sizing of solar-powered airplanes, applicable to MAVs as well as to manned sailplanes, that optimizes the sizing of the different elements. It uses mathematical models, for weight prediction for example, that were studied on a very large range. This allows to clearly point out the problems that occur when scaling down solar MAVs.

20.1 Introduction

The research in bio-inspired robotics is growing indisputably. Examples include fly-inspired optic flow for perception as in Chaps. 3, 5, and 6, artificial nervous systems for control developed through genetic algorithms, flight mechanics based on studies on flapping wings using tiny artificial muscles as in Chap. 16. The autonomous MAVs coming out of this research can rarely be tested more than 15–20 min, simply because in terms of energy storage and flight efficiency, robotics is still far away from biology [10].

A solution to expand this endurance for MAVs is the use of solar energy. With solar cells integrated in their structure and a dedicated electronics called maximum power point tracker (MPPT) to manage them, they would be able to acquire energy from the sun and use it for flight propulsion and control, the eventual surplus being stored for higher power demands.

20.1.1 State of the Art

The history of solar aviation has seen the realization of numerous very successful airplanes powered only with this abundant and free energy [9]. In 1974, two decades after the development of the silicon photovoltaic cell, R.J. Boucher and his team designed the first solar-powered aircraft, which then performed a 20 min flight. The new challenge that fascinated the pioneers was then to achieve manned flight solely powered by the sun. In 1980, this was realized with the Gossamer Penguin, designed by Dr. Paul B. McCready and AeroVironment Inc. Since then, many projects started, most of them in the direction of high-altitude long-endurance platforms with wingspans of several tens of meters. Unfortunately, solar flying platforms below 1 m are far less numerous. A few hobbyists developed such MAVs, like the SolFly, Sol-Mite, and Micro-Mite. In the academic community, Roberts et al. designed the 38 cm wingspan SunBeam [11] and Fuchs and Diepeveen worked on the 77 cm Sun-Surfer. However, they all encountered problems achieving a stable long-duration flight.

20.1.2 Objectives and Structure of this Chapter

This chapter aims at investigating precisely the problems that occur when targeting solar flight at the MAV

A. Noth (✉)
Autonomous Systems Lab, ETHZ, Zürich, Switzerland
e-mail: andre.noth@a3.epfl.ch

D. Floreano et al. (eds.), *Flying Insects and Robots*,
DOI 10.1007/978-3-540-89393-6_20, © Springer-Verlag Berlin Heidelberg 2009

size, by focusing on the global design of such flying platforms. We will not tackle the precise problem of airfoil selection only, or propeller optimization, but rather concentrate on the optimal sizing of all the elements and particularly emphasize the scaling effects. For this purpose, we will introduce the design methodology that was developed within the framework of the Sky-Sailor project[1] at the Autonomous Systems Lab of ETHZ in Zürich. A first example will show how it was applied on the 3.2 m wingspan Sky-Sailor UAV. Then, using the mathematical models developed for each subpart, such as the mass and efficiency of a motor with respect to its power, the advantages and drawbacks of downscaling will be presented. That will allow an adaptation of the parameters used in the methodology in order to design a solar MAV.

20.2 Design Methodology

The methodology that we propose is based on two simple balances:

- Weight balance: the lift force has to be equal to the weight of all the elements constituting the airplane.
- Energy balance: the energy that is collected during a day or the light period from the solar panels has to be equal or higher than the electrical energy needed by the motor during the entire flight.

These two balances are represented in Fig. 20.1 where it is clear that the propulsion group and the airframe cannot be dimensioned without knowing the total mass to lift, but this value is the sum of the masses of all the airplane elements that will be sized according to the energy required by the propulsion group. From here on, and considering the type of mission and the payload to embed, there could be two different methods to solve this loop, i.e., to design the airplane.

[1] http://sky-sailor.epfl.ch/

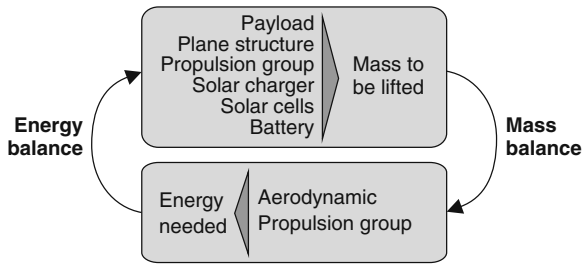

Fig. 20.1 Energy and mass balances

- The ***discrete and iterative approach*** would consist in selecting a first set of components (motor, solar panels, battery, etc.) based on pure estimation of the final required power or on previous designs. Then, having their total mass, the wing surface and propulsion group could be sized. Having chosen a precise motor, gearbox, and propeller, one could calculate the power needed for level flight. This value would then be compared with the power available from the previously selected solar generator, and so on, an iterative process would take place with at each time refining selection, improving the design, ending hopefully with a converging solution.
- The approach used here is an ***analytical and continuous approach*** that consists in describing all the relations between the components with analytical equations using models describing the characteristics of each of them. This method has the benefit of directly providing a unique and optimized design, but requires very good mathematical models. In the present case, an important effort was made to make these models accurate on a very wide range, so that the methodology could be applied to solar MAVs as well as to manned solar airplanes.

The first steps are thus to establish the expression of the power needed for the aircraft in level flight, the solar energy available, and then develop the weight prediction models for all the airplane elements. All the details of these developments can be found in [8] and [9] and are summarized in compact form in Fig. 20.2. It represents the problem of solar airplane conceptual design in a graphical approach and in fact contains the same loop that is depicted in Fig. 20.1 but displayed in a compact mathematical manner.

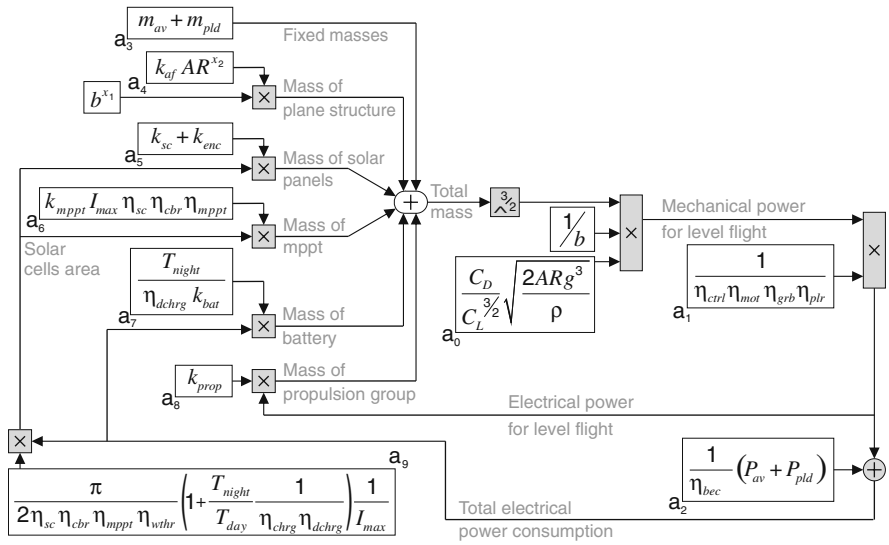

Fig. 20.2 Schematic representation of the design methodology

In order to extract meaningful information, it is necessary, among the 30 parameters that our model contains, to distinguish between three different classes:

- The first group is composed of the parameters which are linked to a technology and are constant or can be regarded as constant for very good design. This is for example the case of motor or propeller efficiencies that should be around 85% when optimized for a specific application [13].
- The second group of parameters is linked to the mission: they are the air density, given by the flight altitude; the day and night duration, depending on the time and the location; and the mass and power consumption of the payload.
- Finally, the last group is composed of the parameters that we vary during the optimization process in order to determine the airplane layout, that is why we should use here the term variable rather than parameter. They are the wingspan and the aspect ratio of the wing.

A complete listing of these parameters is presented in Tables 20.1, 20.2, and 20.3. The values that are mentioned were used for the design of the 3.2 m wingspan Sky-Sailor prototype.

The process to solve the loop analytically is quite simple. Considering the point where the masses of all elements are summed up in Fig. 20.2 and using the substitution variables a_i, we can write

$$\begin{aligned} &m - \underbrace{a_0 a_1 (a_7 + a_8 + a_9 (a_5 + a_6))}_{a_{10}} \frac{1}{b} m^{\frac{3}{2}} \\ &= \underbrace{a_2 (a_7 + a_9 (a_5 + a_6)) + a_3}_{a_{11}} + a_4 b^{x_1} \end{aligned} \tag{20.1}$$

$$m - \underbrace{a_{10} \frac{1}{b}}_{a_{12}} m^{\frac{3}{2}} = \underbrace{a_{11} + a_4 b^{x_1}}_{a_{13}} \tag{20.2}$$

or more compact

$$m - a_{12} m^{\frac{3}{2}} = a_{13} \tag{20.3}$$

Equation (20.3) has only a positive non-complex solution, which makes physical sense, if

$$a_{12}^2 a_{13} \leq \frac{4}{27} \tag{20.4}$$

The conceptual design process can thus be summarized as follows: after having set the mission requirements and chosen the technological parameters, one can try many possible airplane layouts by changing b and AR. The condition on Eq. (20.4) tells directly if the

Table 20.1 Parameters that are constant or assumed constant

Parameter	Value	Unit	Description
C_L	0.8	–	Airfoil lift coefficient
$C_{D\,afl}$	0.013	–	Airfoil drag coefficient
$C_{D\,par}$	0.006	–	Parasitic drag coefficient
e	0.9	–	Oswald's efficiency factor
I_{max}	950	[W/m^2]	Maximum irradiance
K_{bat}	190·3600	[J/kg]	Energy density of Li-Ion
K_{sc}	0.32	[kg/m^2]	Mass density of solar cells
K_{enc}	0.26	[kg/m^2]	Mass density of encapsulation
K_{mppt}	0.00042	[kg/W]	Mass to power ratio of MPPT
K_{prop}	0.0008	[kg/W]	Mass to power ratio of prop. group
K_{af}	0.44/9.81	[kg/m^3]	Structural mass constant
m_{av}	0.15	[kg]	Mass of autopilot system
η_{bec}	0.65	–	Efficiency of step-down converter
η_{sc}	0.169	–	Efficiency of solar cells
η_{cbr}	0.90	–	Efficiency of the curved solar panels
η_{chrg}	0.95	–	Efficiency of battery charge
η_{ctrl}	0.95	–	Efficiency of motor controller
η_{dchrg}	0.95	–	Efficiency of battery discharge
η_{grb}	0.97	–	Efficiency of gearbox
η_{mot}	0.85	–	Efficiency of motor
η_{mppt}	0.97	–	Efficiency of MPPT
η_{plr}	0.85	–	Efficiency of propeller
P_{av}	1.5	[W]	Power of autopilot system
x_1	3.1	–	Airframe mass area exponent
x_2	–0.25	–	Airframe mass aspect ratio exponent

Table 20.2 Parameters determined by the mission

Parameter	Value	Unit	Description
m_{pld}	0.05	[kg]	Payload mass
η_{whtr}	0.7	–	Irradiance margin factor
P_{pld}	0.5	[W]	Payload power consumption
ρ	1.1655	[kg/m^3]	Air density (500 m)
T_{day}	13.2·3600	[s]	Day duration

design is feasible or not with this wingspan and aspect ratio. In the case of a positive answer, the total mass m can be found, which will constitute the starting point for the calculation of the power and characteristics of all the other elements. Hence, this method is not aimed at being used to optimize a precise and local element like the airfoil or the propeller, its objective is rather to help to choose the best combination and size of the different elements.

Table 20.3 Variables linked to the airplane shape

Parameter	Value	Unit	Description
AR	12.9	–	Aspect ratio
b	3.2	[m]	Wingspan
m	2.5	[kg]	Total mass

20.3 Methodology Application: The Sky-Sailor UAV

In order to see how it can be concretely applied, we will present here the example of the Sky-Sailor airplane. The objective here is to design an UAV that can embed a small payload of around 50 g, but that can achieve continuous flight at constant altitude over 24 h using only solar energy. The mission and technological parameters that were used are presented in Tables 20.1, 20.2.

Using these parameters and trying various airplane shapes, i.e., wingspan from 0 to 6 m and different aspect ratios, Eq. (20.4) determines if the solution is feasible, in which case Eq. (20.3) is solved to find the airplane gross mass (Fig. 20.3).

Having found for each possibility the total mass, one can then introduce it in the loop of Fig. 20.2 to calculate precisely all the other airplane characteristics:

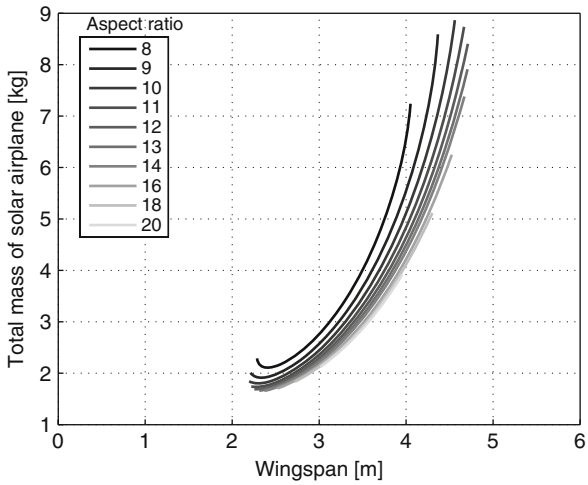

Fig. 20.3 Possible size configurations for a solar UAV embedding a 50 g payload for a 24 h flight depending on the wingspan b and the aspect ratio AR

powers at propeller, gearbox, motor and battery, surface of wing and solar panels, weights of the different subparts and also flying speed (Fig. 20.4).

Finally, depending on the application, a selection criterion will be defined. They can concern speed or wingspan, the UAV being stowed in a limited volume and launched by hand. With the help of the plot of Fig. 20.4, a final configuration will be selected.

In the case of the Sky-Sailor project, a wingspan of 3.2 m and an aspect ratio of 13 were selected, which leads to a theoretical mass of 2.55 kg. It is also interesting to plot the mass distribution in Fig. 20.5, for example, to observe that the battery constitutes more than 40% of the entire weight. Between 2005 and 2007, a fully functional prototype was realized to validate this design methodology (Fig. 20.6). The efficiencies and weight prediction models turned out to be very accurate, resulting in a total airplane mass of 2.506 kg and a total electrical power draw of 14 W for level flight, whereas the predicted power consumption was 14.2 W. The wing is covered by a half square meter of silicon solar cells that offer a maximum power of 90 W at noon in summer.

The prototype was tested successfully in June 2008 during an autonomous flight of more than 27 h with a flight distance of 874 km, using the sun as the only source of energy. This experiment proved the feasibility of continuous flight at constant altitude without using thermal soaring or storing potential energy by gaining altitude in the afternoon. It, however, requires extremely calm wind conditions, a good irradiance during the day, and especially no clouds at sunrise and sunset. Further information concerning this prototype can be found in [8].

20.4 The Pros and Cons of Downscaling

In the last section, we considered the application of our methodology and validated it at the UAV size, but now we can wonder how the feasibility of solar flight evolves with scaling. The analytical character of the design method and its mathematical models allows us to precisely discuss these scaling issues on the different airplane parts, which is the subject of the following subsections.

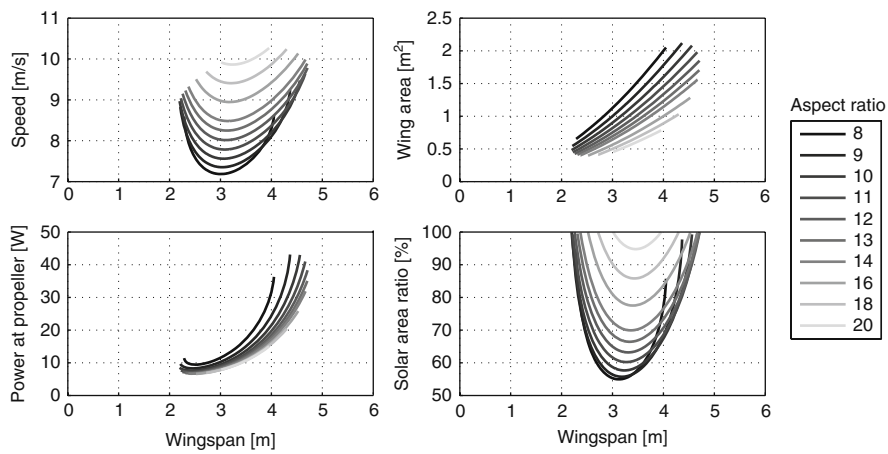

Fig. 20.4 Aircraft and flight characteristics depending on the wingspan b and the aspect ratio AR

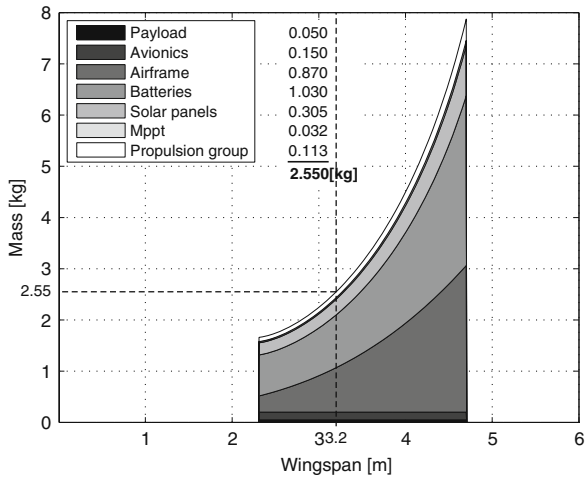

Fig. 20.5 Mass distribution for the solution with AR = 13

20.4.1 Airframe

The airplane structure is the only part that scales down very well. In fact, its weight is proportional to the cube of a reference length, the wingspan for example. This property was highlighted by Tennekes in 1992 who presented, in his book "The simple science of flight" [14], very interesting correlations including insects, birds, and airplanes. He summarized the relations in a log–log diagram named "The Great Flight Diagram" where, following his own words, "everything that can fly" is represented. The result is impressive: 12 orders of magnitude in weight, 4 orders of magnitude in wing loading, and 2 orders of magnitude in cruising speed. From the common fruit fly, *Drosophila melanogaster*, to the boeing 747, all the flying objects follow approximately a line with the following equation:

$$W/S = 47\ W^{1/3} \tag{20.5}$$

This cubic relation was also validated for sailplanes by the author with a database of 515 RC models and manned sailplanes [9]. A first interpolation was achieved to obtain the mean model after which only the best sailplanes, i.e., lighter than this mean model, were kept for a second interpolation. After five iterations of this process, only 5% of the initial database remained to give the 5% best model, represented in Fig. 20.7 with the Great Flight Diagram. Our models are on the upper side of Tennekes curve which means that they are lighter, but at the same time more fragile. On the lower side, one can find the more robust flying systems, ranging from the house flies to combat aircrafts. These are heavier but able to withstand acrobatic maneuvers.

The same figure also contains 86 solar-powered airplanes flown to date. The available solar power relates linearly to the wing surface, thus square with the wingspan. The fact that the aircraft structure weight increases with the cube of the wingspan is a huge problem for large solar airplanes. As a matter of fact, it can be shown mathematically that the feasibility of these large solar airplanes implies a square and not a cubic relation between weight and wingspan [8]. This ideal weight prediction model is represented with the gray region in Fig. 20.7. It explains why existing large solar airplanes tend to get closer to these regions. At these large dimensions, this attempt to reduce mass leads to the construction of very fragile wings, like in the case of the NASA Helios which was destroyed when it fell into the Pacific Ocean on June 26, 2003, due to structural failures. When scaling down, this cubic

Fig. 20.6 The Sky-Sailor prototype held by the author and during a flight

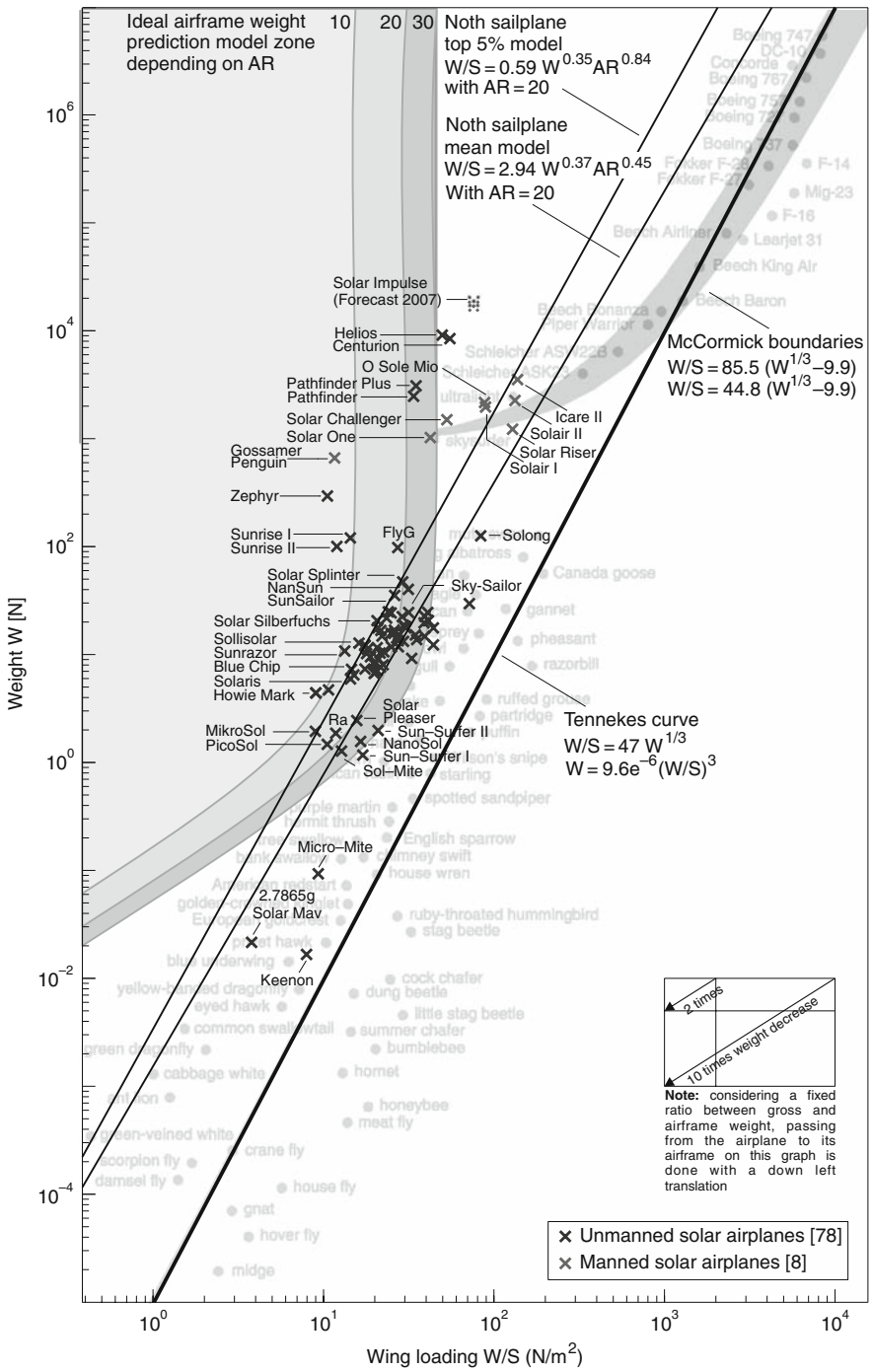

Fig. 20.7 The Great Solar Flight Diagram: improved version of Tennekes Great Flight Diagram [14] showing the cubic relation between weight and wing loading with 86 solar airplanes flown from 1974 to 2008. The McCormick boundaries [6] show the same cubic tendency for manned airplanes with an asymptote representing the weight of an adult. The gray regions represent the zone where the airplane structure should be located to ensure the feasibility of continuous solar flight

law becomes a clear advantage. In fact, dividing the wingspan by a factor of 2 reduces the surface by 4, but the weight of the structure by 8.

Additionally, the structure stiffness and the stress related to the mass scale linearly with the reference length. This is a great advantage for smaller systems which are intrinsically more robust against destruction forces related to their own mass. Also, an MAV has a much higher chance to survive a free fall than a big airplane because of the increasing ratio between air drag

and mass. Nature gives us the example of ants that easily survive a fall from a multi-floor building whereas the elephant is seriously hurt when falling from around 1 m [2].

20.4.2 Low Reynolds Number Airfoil and Propeller

Unfortunately, there are many drawbacks when scaling down an aircraft in size. On the aerodynamic side, it is well known that the lift to drag ratio decreases dramatically for Reynolds number smaller than 10^5 (Fig. 20.8).

That is basically why natural selection made the smallest birds and insects flap their wings, in order to increase Reynolds number. Whereas the lift to drag ratio of the 3.2 m wingspan Sky-Sailor is 24, this value decreases dramatically to 6 for both the Black Widow of AeroVironment [4] and the 2 g Glider of UC Berkeley [16], both in the MAV category. This issue is also discussed in more detail in Chap. 21.

This low Reynolds number effect is negative for the main wing airfoil, but also for the propeller that sees its efficiency decrease dramatically. The measured propeller efficiency of the SunBeam, a 50 cm solar MAV [11], was 58%, which is far away from the 85% of the Sky-Sailor [8]. For the 56.5 g MAV Black Widow, it was clear at the beginning for the builders that an off-the-shelf propeller would lead to a poor efficiency. That is the reason why they designed and molded an optimized propeller with a reported measured efficiency of 80% [4]. More information on the relation between size, power, and turn rate can be found in Chap. 21.

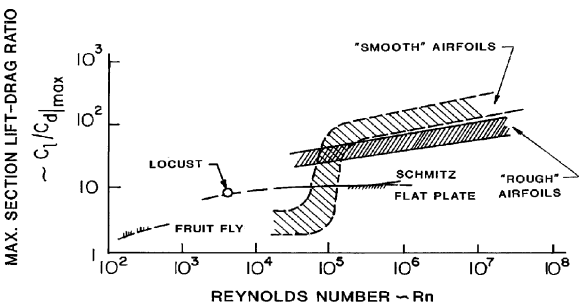

Fig. 20.8 Low Re number performance of smooth and rough airfoils [7]

20.4.3 Actuators

The downscaling of electromagnetical motors is not favorable either. We have studied more than 2000 motors, from 1 mW to 10 kW, and it shows that the power to mass ratio is linear, hobbyist brushless motors being better than the industrial ones as demonstrated in Fig. 20.9. However, Fig. 20.10 shows that the efficiency drops significantly below 1 W. Moreover, the control electronics of the brushless models is slightly more complicated than for the normal DC motors.

Here again, this is confirmed by the Black Widow that has a motor–gearbox efficiency of 50%. This leads to a propulsion group efficiency 40%. It emphasizes the fact that a very important point is the correct matching between motor, gearbox, and propeller. Unfortunately, the market offers far more products for the UAV than for the MAV range. It is thus even more difficult to find a good matching. The only remaining solution is to design and build a dedicated motor, gearbox, and propeller that fit perfectly to the application.

For very low power, it seems that piezoelectric actuators could play an important role as their efficiency, poor compared to traditional electromagnetic motors at big dimensions, turns out to be more efficient than them at low dimensions [15], as the application in Chap. 16 shows. However, their command requires high voltages which induces more complex and heavier control electronics.

Concerning the actuation of the control surfaces, servo motors are generally used for UAVs, but at the MAV size, it is more difficult to find lightweight and still reliable products. Alternative solutions are the use of magnet-in-a-coil actuators [17] such as those used on the MC2 microflyer in Chap. 6 or shape memory alloys [5] like in the case of the gliding robot in Chap. 19.

20.4.4 Solar Cells

Solar cells are also a problem, because they do not scale with the cube of the reference length but with the square. In fact, when reducing the wing surface of an MAV, we can put less cells but the thickness remains the same. Weight percentage then increases as compared to the total MAV mass. Another problem is that

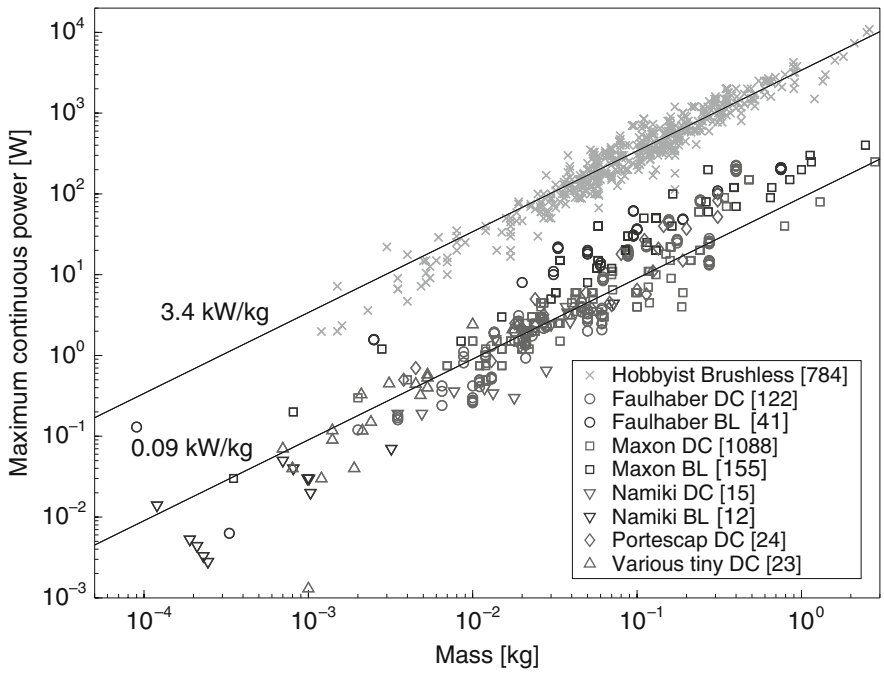

Fig. 20.9 Power to mass ratio for 2264 commercial motors from a database created with the specifications of various manufacturer's products

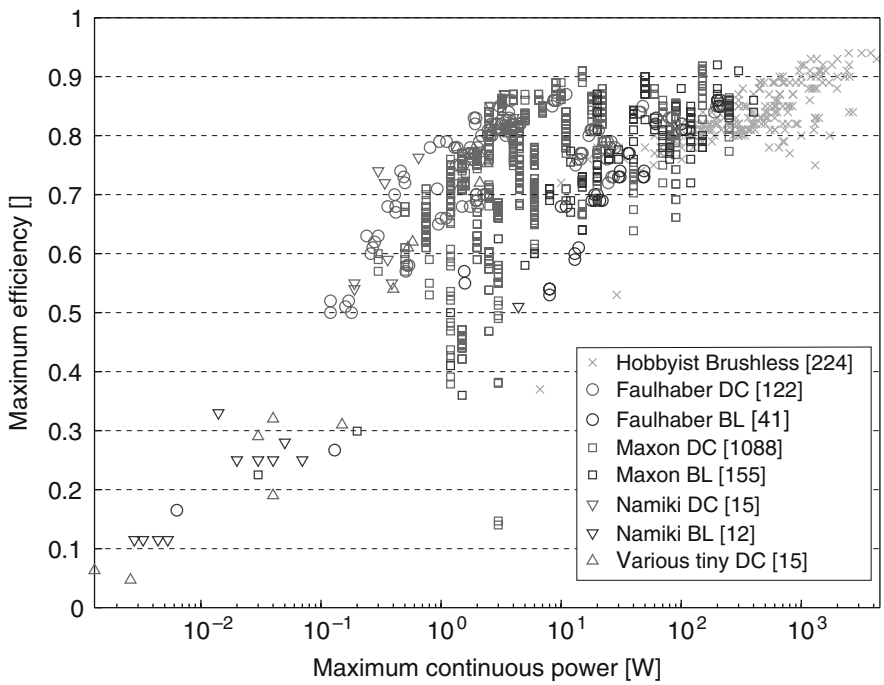

Fig. 20.10 Efficiency of 1672 motors vs maximum continuous power from a database created with the specifications of various manufacturer's products

scaling down an airfoil decreases its curvature radius, making it far more difficult to install the fragile cells on a cambered wing.

A solution to this problem is to place them flat inside the wing, closing the profile with a transparent sheet. This sheet must be non-reflective, otherwise it induces additional losses. Highly flexible solar cells (FlexCell, PowerFilm) can be applied on low curvature radius airfoils, but do not currently have high enough efficiency to be considered for continuous solar flight. They can,

however, be used on an MAV that can recharge its batteries on the ground between two flights [3].

20.4.5 Maximum Power Point Tracker

The MPPT is responsible for interfacing the battery with the solar panels ensuring that they work at the maximum power point. Its efficiency also decreases at low dimensions where the operating voltage is reduced. This loss is due to the diode dropout voltage, which is 0.4 V for good Schottky diodes. In the case of the Sky-Sailor that has a battery voltage of 30 V, this is not critical, but on an MAV powered by a single lithium-ion cell of 3.7 V, this translates into a loss of 11% of the source voltage. This is the reason why in some low-voltage designs, the solar cells are directly connected to the battery, choosing the number of solar cells in series so that their maximum power point voltage corresponds to the battery's nominal voltage.

20.4.6 Energy Storage

On the side of energy storage, high gravimetric energy density lithium-ion or lithium-ion-polymer cells are not easily scalable. Current battery technology is driven by the market of mobile devices; thus, the cells with the best specific energy are always of the 18650 type, a standard size in portable computer battery pack. In 2008, they offered energy densities of up to 240 Wh/kg. They weigh at least 45 g; thus, for a large airplane it is not problematic to use several of them, but they cannot be divided up for tiny MAVs. The only choice is then to select tiny batteries as presented in Chap. 21 where the weight percentage of housing is higher, which inevitably reduces the energy density.

20.4.7 Control

If the MAV is aimed at being autonomous, the development of a navigation and control system becomes very critical at small scales, especially from the sensor side. It is no longer possible to embed GPS or IMU, the smallest of these two devices currently weighing around 10 g including the antenna for the GPS. Hence, the expectations concerning the control capabilities have to be reduced. This limitation forces engineers to develop lightweight and low-power devices to sense the environment, taking inspiration from nature as in Chap. 6 where optical flow is used to avoid walls.

Also, the control of such MAVs itself is more difficult as they are more dynamic than larger UAVs. In fact, if we consider the angular acceleration formula $M = I_\alpha$ and an airplane with a reference length l, the following reasoning can be done; moments on the airplane are the product of length and aerodynamic forces:

$$M \sim l \cdot F \sim l \cdot S \cdot \upsilon^2 \sim l^3 \cdot \upsilon^2 \tag{20.6}$$

In order to find how the speed scales with the reference length, we can use the lift force and put it into equality with the weight, obtaining the flight speed at level flight

$$v = \sqrt{\frac{2\,m\,g}{C_L\,\rho\,S}} \sim \sqrt{\frac{l^3}{l^2}} \sim \sqrt{l} \tag{20.7}$$

Substituting Eq. (20.7) in Eq. (20.6) shows clearly that $M \sim l^4$. Concerning the inertia, we know that

$$I \sim m \cdot l^2 \sim l^5 \tag{20.8}$$

Considering again the angular acceleration formula, we can write

$$\alpha = \frac{M}{I} \sim \frac{l^4}{l^5} \sim \frac{1}{l} \tag{20.9}$$

This result proves that the smaller an aerial vehicle is, the more dynamic it is. Consequently in the case of MAVs, it tends to be more difficult to maintain a constant angle of attack and thus stay at an optimal angle where an aerodynamic characteristic like the lift to drag ratio is the highest. Other very interesting laws of similitude for small-size robots and problems that they induce are discussed by Caprari in [2].

20.5 Application Example on a Solar MAV

After having seen the many problems occurring when scaling down a solar airplane, we will try to adapt the

Table 20.4 Parameter changes at the MAV size

Parameter	Value	Unit	Description
C_L	0.5	–	Airfoil lift coefficient
C_{Dafl}	0.05	–	Airfoil drag coefficient
e	0.6	–	Oswald's efficiency factor
E_{af}	5.58/9.81	[kg/m^3]	Structural mass constant
m_{av}	0.005	[kg]	Mass of autopilot system
η_{grb}	0.81	–	Efficiency of gearbox
η_{mot}	0.62	–	Efficiency of motor
η_{plr}	0.80	–	Efficiency of propeller
P_{av}	0.1	[W]	Power of autopilot system
x_1	3.18	–	Airframe mass area exponent
x_2	–0.88	–	Airframe mass aspect ratio exponent
m_{pld}	0.01	[kg]	Payload mass
P_{pld}	0.00	[W]	Payload power consumption

parameters that were used for the Sky-Sailor to the MAV size, i.e., for aircrafts with a span of less than 6 in. (15.24 cm) and a mass of less than 100 g [4]. Basically, the aerodynamics coefficients (C_L, C_D) quality is reduced, as well as the propulsion group elements efficiencies. The new values were taken from the Sun-Beam and the Black Widow case studies [11,4]. The induced drag is taken into account this time with an Oswald factor of 0.6. Concerning the airframe weight prediction, the mean model of Fig. 20.7 is considered instead of the 5% model. Of course, the mission objectives is also reduced in terms of payload mass and power, as well as the avionics system. All these changes are summarized in Table 20.4.

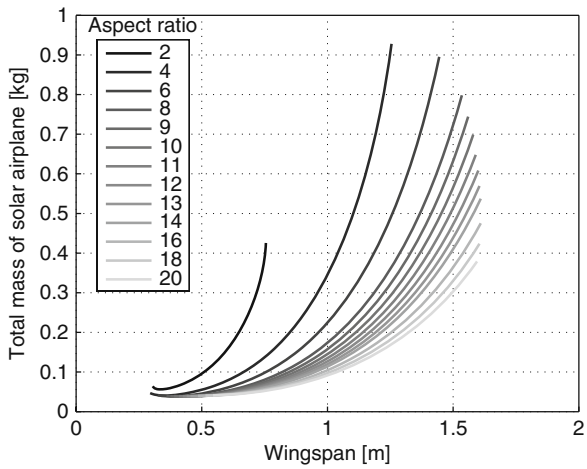

Fig. 20.11 Possible size configurations for a mini Solar UAV embedding a 10 g payload for a daily flight depending on the wingspan b and the aspect ratio AR

Using these new parameters, the first result is that it is impossible to find a configuration for which it is possible to fly continuously over 24 h in the MAV size, even without payload. This accomplishment is already a real challenge at the UAV scale, thus, with the lower efficiencies and aerodynamic problems at MAV size, it becomes understandable.

The methodology can be slightly modified to design an airplane that flies only during the day. For this purpose, we can set $T_{night} = 0$ and give T_{day} any value higher than zero. A quick look at Fig. 20.2 to consider the influence of this change shows that no battery will be considered and the area of solar cells will be lower, which is logical as no battery needs to be charged during the flight. In this case when we consider a mean irradiance, the value of I_{max} has to be multiplied by $\pi/2$, because we consider now an instantaneous irradiance and no more a sinusoidal irradiance model on the entire day [8].

The results show that the minimum airplane wingspan is around 30 cm. Following the definition of an MAV cited above with a span limited to 15.24 cm, it cannot be considered an MAV. It is also not wise to choose a wingspan at the limit of the solution domain because a small change in one of the models, for example, a slightly heavier airframe, and the solution is no longer feasible (Fig. 20.11). Also, an airplane with a very low aspect ratio like the black widow will have a higher dynamic around the roll axis than for a higher aspect ratio. Taking this into account and considering a low speed as selection criteria (Fig. 20.12), a possible solution would be an airplane with an aspect ratio of 10 and a wingspan of 80 cm (Fig. 20.13).

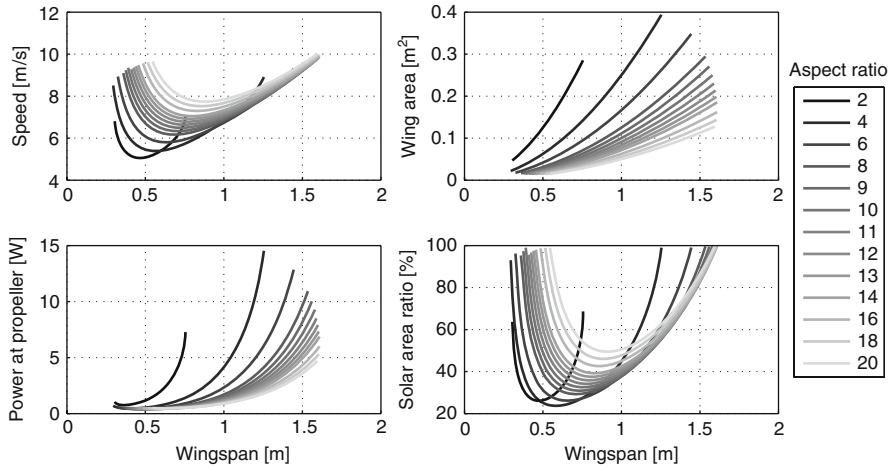

Fig. 20.12 Aircraft and flight characteristics depending on the wingspan b and the aspect ratio AR

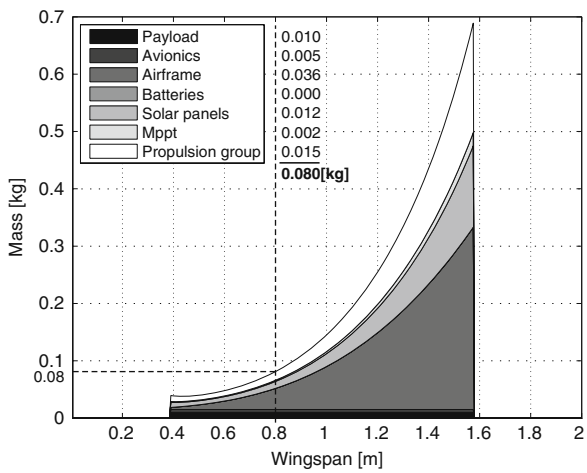

Fig. 20.13 Mass distribution for the solution with AR = 10

Two successive prototypes with a wingspan of 77 cm, named Sun-Surfer 1 & 2, were realized (Fig. 20.14). They emphasized all the problems that were mentioned above, especially the lack of choice in commercially available motors, gearboxes, and propellers, and the low performances of the existing ones. The study also focused on the various airframe construction techniques and ended with the conclusion that the spar and balsa wood rips are lighter than hot wire cut foam or molding methods, even if these latter offer the advantage to be able to get the solar cells molded in the wing without any need of other encapsulation. Finally, both airplanes were tested with a small battery for the launch phase. The propulsion group being less efficient than expected because of a non-optimal matching of commercially available parts, the solar power was not high enough to fly on solar energy only, but rather only increased the autonomy of the battery.

20.6 Conclusion

The development of solar airplanes has seen the realization of many prototypes bigger than a meter, but investigations into their feasibility below this limit are

Fig. 20.14 The two successive versions of Sun-Surfer solar-powered airplanes in flight

very rare. In this chapter, a very simple methodology was developed for the design of this particular type of flying platform, focusing particularly on models with a wingspan below 1 m.

Unfortunately, downscaling introduces many problems which makes the realization of an efficient solar-only MAV impossible at this time. Existing models use a battery coupled to solar cells that only increase the flight time. The main limitations are the low efficiencies of the propulsion group and the deterioration of the aerodynamics characteristics, due to low Reynolds numbers. Additionally, the choice of components, i.e., motor, propellers, batteries, etc., on the market is very poor at this size so it turns out that the realization of a solar MAV first requires a careful design and the manufacturing of dedicated parts specifically for the application. Finally, the design of solar-powered MAVs also requires major improvements on the side of flexible and efficient solar cells, small and high energy density batteries, and lightweight sensors and actuators.

For many of these issues that prevent us to build an MAV with a size of a few centimeters and a reasonable autonomy, a quick look at insects shows us that biology is still far ahead from science. One flagrant example that illustrates this fact is energy storage, where sugar has 20 times more specific energy than the best currently available lithium-ion technology. It will thus require several more decades to be able to compete with nature.

Acknowledgments The authors would like to thank Walter Engel for the outstanding contributions on the realization of the Sky-Sailor prototype and also Niels Diepeveen and Beat Fuchs for their work on the two successive versions of Sun-Surfer.

References

1. Bouabdallah, S., Bermes, C., Schafroth, D., Siegwart, R.: From the Test-benches to the First Prototype of muFly Micro Coaxial Helicopter. Accepted for the 2008 International Symposium on Unmanned Aerial Vehicles (2008)
2. Caprari, G., Estier, T., Siegwart, R.: Fascination of Down Scaling – Alice the Sugar Cube Robot. Journal of Micromechatronics **1**, 177–189(13) (1 July 2001)
3. Fuchs, J.P.: Solar Cell System for the Microglider. Bachelor Thesis, Laboratory of Intelligent Systems, EPFL, Lausanne (2008)
4. Grasmeyer, J.M., Keennon, M.T.: Development of the Black Widow Micro Air Vehicle. Proceedings of the 39th AIAA Aerospace Sciences Meeting and Exhibit, AIAA-2001–0127. Reno, NV, USA (2001)
5. Kovac, M., Guignard, A., Nicoud, J.D., Zufferey, J.C., Floreano, D.: A 1.5 g SMA-Actuated Microglider Looking for the Light. 2007 IEEE International Conference on Robotics and Automation pp. 367–372 (10–14 April 2007)
6. McCormick, B.W.: Aerodynamics, Aeronautics, and Flight Mechanics. John Wiley, New-York (1995)
7. McMasters, J.H., Henderson, M.L.: Low Speed Single Element Airfoil Synthesis. Technical Soaring **6**(2), 1–21 (1980)
8. Noth, A.: Design of Solar Powered Airplanes for Continuous Flight. Ph.D. thesis, Autonomous Systems Lab, ETHZ, Zürich (2008)
9. Noth, A., Siegwart, R., Engel, W.: Autonomous Solar UAV for Sustainable Flight. In: K.P. Valavanis (ed.) Advances in Unmanned Aerial Vehicles, State of the Art and the Road to Autonomy, *Intelligent Systems, Control and Automation: Science and Engineering*, vol. 33, pp. 377–405. Springer Verlag (2007)
10. Pines, D.J., Bohorquez, F.: Challenges Facing Future Micro-Air-Vehicle Development. Journal of Aircraft **43**(2), 290–305 (2006)
11. Roberts, C., Vaughan, M., Bowman, W.J.: Development of a Solar Powered Micro Air Vehicle. Proceedings of the 40th Aerospace Sciences Meeting and Exhibit, AIAA 2002–0703. Reno, Nevada, USA (2002)
12. Shyy, W., Berg, M., Ljungqvist, D.: Flapping and Flexible Wings for Biological and Micro Air Vehicles. Progress in Aerospace Sciences **35**, 455–505 (July 1999)
13. Stadt Ulm, Autorengruppe: Fliegen mit Licht, Dokumentation über solares Fliegen und den Solarflugzeugwettbewerb Berblinger 1996 der Stadt Ulm. Süddeutsche Verlagsgesellschaft Ulm, Ulm (1996)
14. Tennekes, H.: The Simple Science of Flight – From Insects to Jumbo Jets. MIT Press, Cambridge, Massachusetts, USA (1992)
15. Uchino, K.: Piezoelectric Actuators 2006. Journal of Electroceramics, in collection Chemistry and Materials Science (2007)
16. Wood, R.J., Avadhanula, S., Steltz, E., Seeman, M., Entwistle, J., Bachrach, A., Barrows, G., Sanders, S., Fearing, R.S.: Design, Fabrication and Initial Results of a 2 g Autonomous Glider. Industrial Electronics Society, 2005. IECON 2005. 31st Annual Conference of IEEE (6–10 November 2005)
17. Zufferey, J.C., Klaptocz, A., Beyeler, A., Nicoud, J.D., Floreano, D.: A 10-gram Microflyer for Vision-based Indoor Navigation. In: Proc. of the IEEE/RSJ International Conference on Intelligent Robots and Systems (IROS'2006), pp. 3267–3272. Beijing, China (2006)